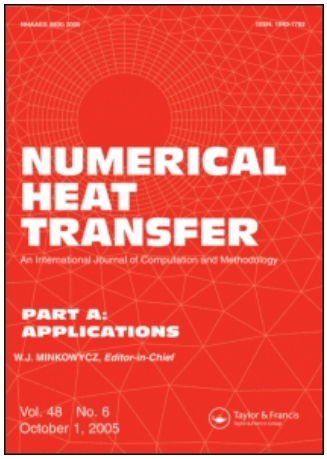

Numerical Heat Transfer, Part A: Applications
An International Journal of Computation and Methodology
Publication details, including instructions for authors and subscription information:
http://www.informaworld.com/smpp/title~content=t713657973

Effect of Surface Radiation on Natural Convection in Parabolic Enclosures

Gerardo Diaz [a]; Roland Winston [a]
[a] School of Engineering, University of California Merced, Merced, California, USA

Online Publication Date: 01 January 2008
To cite this Article: Diaz, Gerardo and Winston, Roland (2008) 'Effect of Surface Radiation on Natural Convection in Parabolic Enclosures', Numerical Heat Transfer, Part A: Applications, 53:9, 891 - 906
To link to this article: DOI: 10.1080/10407780701789518
URL: http://dx.doi.org/10.1080/10407780701789518

Numerical Heat Transfer, Part A, 53: 891–906, 2008

ISSN: 1040-7782 print/1521-0634 online
DOI: 10.1080/10407780701789518

EFFECT OF SURFACE RADIATION ON NATURAL CONVECTION IN PARABOLIC ENCLOSURES

Gerardo Diaz and Roland Winston
School of Engineering, University of California Merced, Merced, California, USA

The interaction of natural convection and surface radiation in two-dimensional parabolic cavities heated from below with insulated walls and flat top and bottom walls is studied numerically. The shape of the cavities arises from the design of non-imaging optics-based compound parabolic concentrators (CPC). A numerical model based on finite differences is developed to solve the mass, momentum, and energy equations. A coordinate transformation is used to map the parabolic shape into a rectangular domain where the governing equations are solved. The results show that surface radiation significantly changes the temperature distribution and local Nusselt number inside the parabolic enclosure. Solutions are obtained for two different parabolic geometries that correspond to two different levels of concentration.

1. INTRODUCTION

This study is part of a research program that focuses in understanding the interaction of heat transfer modes inside parabolic enclosures as found in compound parabolic concentrators. Specifically, the effect of surface radiation on laminar natural convection in an air-filled two-dimensional parabolic cavity is analyzed as a non-rectangular enclosure heated from below.

Natural convection in differentially heated square enclosures has been studied extensively. De Val Davis [1] obtained a benchmark numerical solution of buoyancy-driven flow in a square cavity with vertical walls at different temperatures and adiabatic horizontal walls. De Val Davis and Jones [2] presented a comparison of different contributed solutions to the same problem. These solutions covered the range of Rayleigh numbers between 10^3 to 10^6. More recent contributions include a new benchmark quality solution by means of discrete singular convolution [3], steady-state and transient solutions using a fourth order momentum equation [4], and a study of free convective laminar flow with and without internal heat generation in rectangular enclosures of different aspect rations at various angles of inclination [5].

The effect of surface radiation and natural convection has also been analyzed for regular geometries. Balaji and Venkateshan [6] showed that the Nusselt number distribution clearly shows that surface radiation leads to a drop in the convective

Received 4 April 2007; accepted 19 September 2007.
Address correspondence to Gerardo Diaz, School of Engineering, University of California Merced, P.O. Box 2039, Merced, CA 95344, USA. E-mail: gdiaz@ucmerced.edu

NOMENCLATURE

a	parameter for parabola	x	horizontal coordinate, m
$F_{i,j}$	view factor between segments i and j	Y	dimensionless vertical coordinate
G	dimensionless radiosity	y	vertical coordinate, m
g	acceleration of gravity, $\mathrm{m\,s^{-1}}$	ϵ	emissivity
Gr	Grashof number	ζ	dimensionless transformed coordinate
H	height of cavity, m	η	dimensionless transformed coordinate
h	heat transfer coefficient, $\mathrm{Wm^{-2}\,K^{-1}}$	θ	dimensionless temperature
		θ_0	temperature ratio $T_0/(T_H - T_C)$
k	thermal conductivity, $\mathrm{Wm^{-1}\,K^{-1}}$	σ	Stefan-Boltzmann constant
Nr	conduction-radiation number $(\sigma T_H^4 H/(k(T_H - T_C)))$	τ	dimensionless time
		ϕ	half acceptance angle
q_r	dimensionless radiant heat flux	ω	dimensionless vorticity
Nu	Nusselt number	ψ	dimensionless stream function
Pr	Prandtl number		
Ra	Rayleigh number	**Subscripts**	
T	temperature, K	C	cold wall
T_0	reference temperature $(T_H + T_C)/2$	c	convection
t	time, s	H	hot wall
U	dimensionless velocity in X direction	i	i node
V	dimensionless velocity in Y direction	j	j node
X	dimensionless horizontal coordinate	r	radiation

component. The reduction is compensated by the radiative heat transfer between the hot and cold walls. Akiyama and Chong [7] reported that in the presence of surface radiation, the value of the convection Nusselt number can change but the actual value of the emissivity does not have a large effect on the change. On the other hand, the radiative Nusselt number increases strongly with the increase of emissivity. In a more recent work Ridouane et al. [8] analyzed the interaction between natural convection and radiation in a square cavity heated from below. They found that for an emissivity value greater than 0.22 the type of bicellular solution characterized by the presence of two horizontal cells no longer appears. They also reported that for the unicellular solution, the critical Rayleigh number decreases by increasing the emissivity. Two years later, Ridouane et al. [9] showed that for multiple solutions, a single cell flow transfers more heat than a bicellular flow by as much as 30%. They also reported periodic solutions during the transition from bicellular flow to unicellular flow. The effect on flow stability of diffusely emitting walls in a rectangular cavity at different emissivity values is analyzed numerically by Jaballah et al. [10], and a numerical analysis of the interaction of natural convection and radiation in saturated porous media is reported in [11].

Several natural convection studies have also been published for differentially heated non-rectangular cavities. Date [12] analyzed the natural convection heat transfer in horizontal annulus. It was found that the available generalized correlations for horizontal pressured heavy water reactors overpredicted the numerical results. Wansophark et al. [13] utilized an upwind finite element method to analyze the conjugate heat transfer problem. Other authors have utilized coordinate transformations to solve the governing equations. Badr and Shamsher [14] analyzed the free convection heat transfer from a horizontal elliptic cylinder. The governing

equations were transformed to the elliptic coordinate system. Good agreement was found with theoretical and experimental data available. Other natural convection studies that include coordinate transformations include the works by Karyakin [15] for prismatic enclosures of arbitrary cross section, Lee [16] for convective fluid motion in a trapezoidal enclosure, and Aydemir et al. [17] for free convection in horizontal cylinders. The heat transfer by natural convection has also been studied for parabolic solar concentrators. Abdel-Khalik et al. [18] used finite elements to obtain the flow patterns and Nusselt numbers in non-imaging-optics based compound parabolic concentrators operating in the range of Rayleigh numbers between 2.0×10^3 to 1.3×10^6. They considered full and truncated CPCs in their analysis. Tatara and Thodos [19] provided an experimental study of natural convection in a CPC. A correlation for the Nusselt number in the aperture was developed based on their measurements. The predictions obtained with their correlation tend to be lower than other available correlations by about 15%. The reason for the discrepancy is due to the conductive sidewall effects that were not considered in the development of the correlation. Another experimental study of free convection in a CPC with a cylindrical absorber was presented by Chew et al. [20]. Different cavity heights were tested and the results were compared against a numerical simulation performed by the same authors. Good agreement was obtained between the numerical results and experimental data although the range of overlap was small because stable numerical results could not be obtained at high Grashof numbers. A correlation that includes the effects of height and width of the collector was developed. Combined effects of natural convection and radiation in non-rectangular geometries are reported in [21] and [22].

This article analyzes the coupling of natural convection and radiation inside the non-rectangular enclosure of a non-imaging-optics-based solar concentrator first proposed by Winston [23]. The enclosure is formed by the space in between the aperture and the flat absorber as shown in Figure 1*a*.

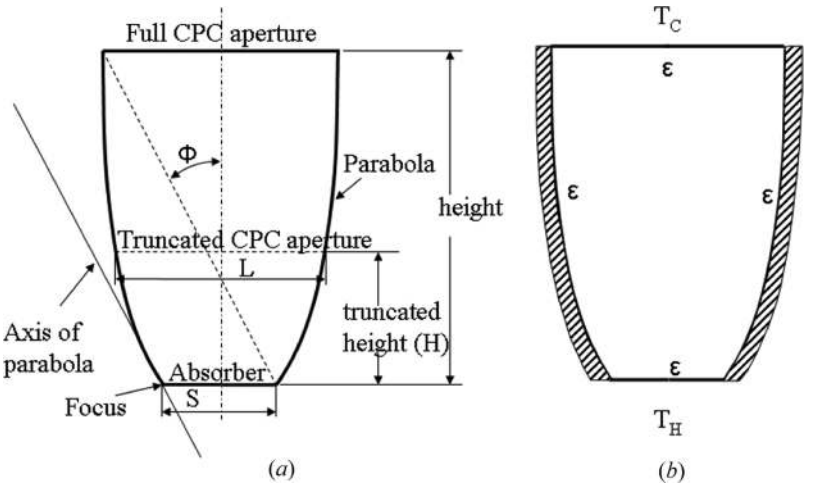

Figure 1. Compound parabolic concentrator cavity.

2. MATHEMATICAL MODEL

2.1. Governing Equations

The two-dimensional laminar Navier-Stokes equations are written in terms of the vorticity-stream function formulation using the Boussinesq approximation. A radiatively nonparticipating medium is used for the simulations and all surfaces are considered as being gray. The governing equations become
Vorticity

$$\frac{\partial \omega}{\partial \tau} + U\frac{\partial \omega}{\partial X} + V\frac{\partial \omega}{\partial Y} = -\mathrm{PrRa}\frac{\partial \theta}{\partial X} + \mathrm{Pr}\left(\frac{\partial^2 \omega}{\partial X^2} + \frac{\partial^2 \omega}{\partial Y^2}\right) \tag{1}$$

Energy

$$\frac{\partial \theta}{\partial \tau} + U\frac{\partial \theta}{\partial X} + V\frac{\partial \theta}{\partial Y} = \frac{\partial^2 \theta}{\partial X^2} + \frac{\partial^2 \theta}{\partial Y^2} \tag{2}$$

Stream function

$$-\omega = \frac{\partial^2 \psi}{\partial X^2} + \frac{\partial^2 \psi}{\partial Y^2} \tag{3}$$

where

$$U = \frac{\partial \psi}{\partial Y} \quad V = -\frac{\partial \psi}{\partial X} \tag{4}$$

$X = \frac{x}{H}$, $Y = \frac{y}{H}$, $\theta = \frac{T - T_C}{T_H - T_C}$, $\mathrm{Gr} = \frac{g\beta \Delta T H^3}{\nu^2}$, $\mathrm{Ra} = \mathrm{PrGr}$, and $\tau = \frac{\nu}{H^2}\sqrt{\mathrm{Gr}}t$.
The dimensionless radiant heat flux is calculated as

$$q_r = \epsilon_i \left[\left(\frac{T_i}{T_H}\right)^4 - \sum_j F_{ij} G_j\right] \tag{5}$$

The nondimensional radiosity equation for the ith element of each wall is given by

$$G_i = (1 - \epsilon_i)\sum_j F_{ij} G_j + \epsilon_i \left(\frac{T_i}{T_H}\right)^4 \tag{6}$$

where the view factors F_{ij} between the elements are obtained using the crossed string method described in Hottel and Sarofim [24].

2.2. Coordinate Transformation

In order to obtain a solution of the fluid flow and heat transfer rate inside the non-rectangular enclosure, we apply a coordinate transformation that maps a parabolic domain into a rectangular domain.

For a parabola $Y = aX^2,\ Y > 0,\ a > 0$, we use

$$\zeta = \frac{X}{\sqrt{Y/a}} \quad \eta = Y \tag{7}$$

By applying this transformation, the governing equations become
Vorticity

$$\frac{\partial \omega}{\partial \tau} + \sqrt{\frac{a}{\eta}}\left(\frac{\partial \psi}{\partial \eta}\frac{\partial \omega}{\partial \zeta} - \frac{\partial \psi}{\partial \zeta}\frac{\partial \omega}{\eta}\right) = -\sqrt{\frac{a}{\eta}}\mathrm{PrRa}\frac{\partial \theta}{\partial \zeta} + \mathrm{Pr}\nabla^2\omega \tag{8}$$

Energy

$$\frac{\partial \theta}{\partial \tau} + \sqrt{\frac{a}{\eta}}\left(\frac{\partial \psi}{\partial \eta}\frac{\partial \theta}{\partial \zeta} - \frac{\partial \psi}{\partial \zeta}\frac{\partial \theta}{\partial \eta}\right) = \nabla^2\theta \tag{9}$$

Stream function

$$-\omega = \nabla^2\psi \tag{10}$$

where

$$\nabla^2 = \frac{1}{\eta}\left(a + \frac{\zeta^2}{4\eta}\right)\frac{\partial^2}{\partial \zeta^2} + \frac{3}{4}\frac{\partial}{\partial \zeta} - \frac{\zeta}{\eta}\frac{\partial^2}{\partial \zeta \partial \eta} + \frac{\partial^2}{\partial \eta^2} \tag{11}$$

The boundary conditions also need to be transformed to the computational domain. The stream function ψ is zero on all the surfaces. The temperature θ is equal to one at the bottom of the cavity ($\eta = 0$) and zero at the top ($\eta = 1$). For the adiabatic vertical walls

$$\frac{\partial \theta}{\partial \zeta} + N_r q_r = 0 \tag{12}$$

where $Nr = \sigma T_H^4 H/(k(T_H - T_C))$. The boundary conditions for the vorticity are obtained from Eq. (10) evaluated at the walls.

2.3. Nusselt Number

The average Nusselt number corresponds to the sum of the convective and radiative components

$$\overline{\mathrm{Nu}} = \overline{\mathrm{Nu}}_c + \overline{\mathrm{Nu}}_r \tag{13}$$

Once a solution is obtained in the computational domain, the results of temperature, vorticity, and stream function are mapped back to the dimensionless

parabolic domain. The expression used for the average convective Nusselt number is

$$\overline{\mathrm{Nu}_c} = \frac{1}{l}\int_0^l -\frac{\partial\theta}{\partial Y}\bigg|_{\text{wall}} dX \tag{14}$$

where l is calculated for the cold or hot wall as $l = \int_{\text{wall}} dX$.

The radiative Nusselt number is obtained as follows:

$$\overline{\mathrm{Nu}_r} = \frac{1}{l}\int_0^l N_r q_r\Big|_{\text{wall}} dX \tag{15}$$

where the view factors used to calculate q_r are calculated from the parabolic shape.

3. NUMERICAL MODEL

The governing equations are discretized and solved using an explicit method. Second order approximations are used for the first and second order derivatives. This study concentrated in steady state solutions so the stream function equation is solved by introducing a transient term in Eq. (10) Coefficients α_ω, α_ψ, and α_θ were also introduced to improve the stability of the solution [1].

4. RESULTS AND DISCUSSION

4.1. Model Validation

The natural convection model is first validated against a benchmark solution in cartesian coordinates. A differentially heated square cavity with adiabatic horizontal walls and constant temperature vertical walls, as described by De Val Davis [1], was used to validate the simulations. No radiation effects were considered in this case. The range of Rayleigh numbers covered the range between 10^3 and 10^6 to remain within the laminar convection regime. As shown in Table 1, the maximum error obtained for the maximum value of the stream function, $|\psi_{\max}|$, with respect to the benchmark solution is 1.02% and a 0.57% was obtained for the average Nusselt number at the hot vertical wall. A 41×41 nodes grid was used to obtain these results based on a grid independence study.

Table 1. Validation of model in Cartesian coordinates

Ra	ϵ	Present $\lvert\psi_{\max}\rvert$	De Vahl Davis $\lvert\psi_{\max}\rvert$	Error %	Present $\overline{\mathrm{Nu}}$	De Vahl Davis $\overline{\mathrm{Nu}}$	Error %
10^3	0	1.172	1.174	−0.17	1.119	1.116	0.27
10^4	0	5.046	5.098	−1.02	2.254	2.242	0.54
10^5	0	9.550	9.644	−0.97	4.545	4.523	0.49
10^6	0	16.807	16.961	−0.91	8.979	8.928	0.57

Table 2. Grid independence for $Ra = 1.0 \times 10^6$, $\epsilon = 1$

Grid	$\lvert\psi_{max}\rvert$	$\overline{Nu_c}$	$\overline{Nu_r}$
31×31	20.210	7.621	15.001
51×51	20.226	7.663	15.083
81×81	20.298	7.709	15.131
101×101	20.326	7.724	15.148

Grid independence was also tested for the case of combined radiation and convection in a square enclosure. Table 2 shows the values obtained for $|\psi_{max}|$, the average convective Nusselt number, $\overline{Nu_c}$, and the average radiative Nusselt number, $\overline{Nu_r}$, for different grid sizes at a constant Rayleigh number $Ra = 1.0 \times 10^6$ and $\epsilon = 1$. The maximum differences in the values obtained with different grids were within 0.57% for $|\psi_{max}|$, 1.33% for $\overline{Nu_c}$, and 0.96% for $\overline{Nu_r}$. Based on the results shown in Table 2 we chose a grid size of 51×51 nodes as a good balance between accuracy and speed of computation.

The model for the interaction between surface radiation and natural convection was validated against the solutions obtained by Akiyama and Chong [7] for a square cavity. Figure 2*a* shows the comparison of the average convective Nusselt number for the hot and cold walls against the results in [7] for a range of Rayleigh numbers between 10^3 and 10^6. Results for $\epsilon = 0$ and $\epsilon = 1$ are shown in this figure. The maximum error for $\overline{Nu_c}$ with no radiation is 4.2% and with radiation is 5.7%. The maximum error in the average radiative Nusselt number, shown in Figure 2*b*, is 1.53%. Figure 3 shows the effect of surface radiation on the streamlines and temperature profile for $Ra = 1.0 \times 10^6$. Figures 3*a* and 3*c* correspond to the streamlines and temperature profile for $\epsilon = 0$, respectively. Figures 3*b* and 3*d* show the streamlines and temperature profile for $\epsilon = 1$, respectively. As shown in the figure, surface radiation has a strong effect on the flow and temperature profile inside the square cavity.

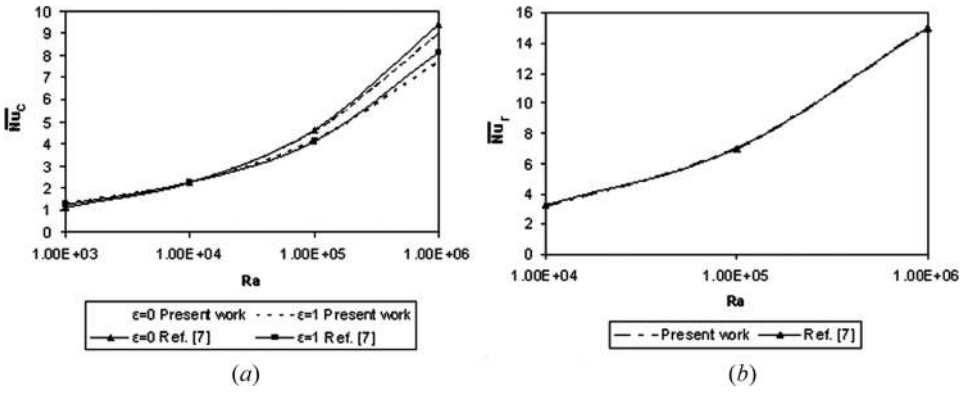

Figure 2. Comparison of convective and radiative Nusselt numbers. Ra between 10^3 and 10^6 and $\epsilon = 0$ or 1.

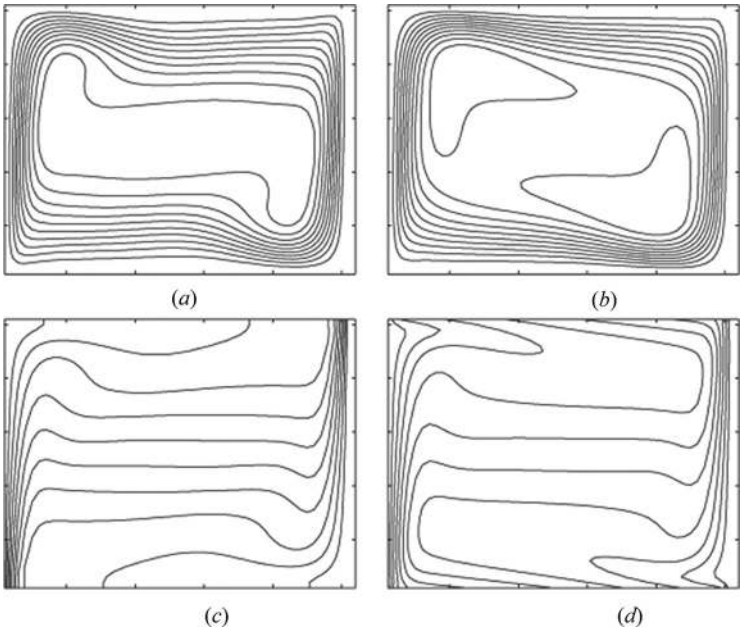

Figure 3. Effect of surface radiation on temperature and streamlines ($T_0 = 293.5$, $\mathrm{Ra} = 10^6$, $\theta_0 = 29.35$). (*a*) Streamlines with $\epsilon = 0$, (*b*) streamlines with $\epsilon = 1$, (*c*) temperature with $\epsilon = 0$, and (*d*) temperature with $\epsilon = 1$.

So far the code has been validated with respect to natural convection and radiation effects in square cavities. We proceed now to simulate the parabolic domain by means of introducing the coordinate transformation described in section 2.2.

4.2. Parabolic Cavity

The governing equations and boundary conditions were transformed to simulate the flow and heat transfer inside a parabolic shape as depicted in Figure 1*a*. The vertical walls were considered adiabatic and the flat absorber, at the bottom, was modeled with a uniform temperature that is higher than the aperture temperature at the top of the cavity. The level of concentration of the collector can be modified by changing the geometry of the parabola. The level of performance is not significantly reduced by truncating a portion of the height of the concentrator [18]. Table 3 shows the geometrical parameters for truncated CPC cavities with one third of the full height of the concentrator. The geometries can be closely approximated by a parabola of the form $Y - Y_0 = aX^2$. The values of a and Y_0 are also shown in Table 3.

Since the geometry of the cavity changes with the level of concentration, we tested for grid independence at two different levels of concentration, (i.e., C2 and C4). Table 4 shows the comparison of the average convection Nusselt number for the hot and cold walls. Four different grid sizes were tested for natural convection with

Table 3. Geometrical parameters for truncated CPC cavity

Concentration, C	ϕ	H/L	H/S	a	Y_0
2.0	30.0°	0.523	0.866	1.78887	0.656873
4.0	14.5°	1.009	3.227	4.55452	0.142635

no radiation effects at $\mathrm{Ra} = 1.0 \times 10^5$. A good compromise between accuracy and computational time is obtained with a grid size of 41×81 which gives a maximum percentage error of 1.28% with respect to the finest grid tested. As a mean of validation of the transformed equations, we compared the results of pure natural convection for levels of concentration C2 and C4 with correlations obtained by Hollands et al. [25, 26] and Holman [27] for horizontal plates heated from below. The correlation developed by Iyican et al. [28] for trapezoidal enclosures was also used for comparison. Figure 4 shows that the onset of natural convection is delayed by the level of concentration in the collector. As the concentration level increases so does the aspect ratio of the cavity and it takes a larger temperature difference (or a higher Rayleigh number) to establish convection [29]. The effect of the walls of the cavity also plays a roll in delaying the onset of motion of the fluid. The suppression of convection at higher concentration levels is in agreement with the results obtained in [18]. At Rayleigh numbers larger than 10^5 the Nusselt number evaluated at the hot wall of cavities C2 and C4 falls in between the Nusselt number obtained with the correlation for the trapezoidal cavity [28] and the horizontal plates heated from below [25, 27].

4.2.1. Effect of Radiation. The effect of radiation on the convective and radiative Nusselt numbers is investigated in this section. The average value of the Nusselt number calculated at the hot and cold walls was used for the analysis. The Rayleigh number was varied from 10^3 to 10^6 keeping the reference temperature at an arbitrary value of $T_0 = 293.5\,\mathrm{K}$ with the temperature ratio at $\theta_0 = 2.935$. Simulations were performed for cavities with levels of concentration C2 and C4. The effect of radiation was studied by comparing the results obtained with $\epsilon = 0$ and $\epsilon = 1$. In order to limit the number of cases, the emissivity has been considered the same for all walls, as depicted in Figure 1*b*. Figure 5*a* shows the comparison of the average convective Nusselt number for pure natural convection and natural convection with radiation for a level of concentration C2. It is observed that as the Rayleigh number increases the value of $\overline{\mathrm{Nu}_c}$ is slightly lower for $\epsilon = 1$ with respect to $\epsilon = 0$. At $\mathrm{Ra} = 10^6$ the difference in $\overline{\mathrm{Nu}_c}$ is 5.4%. This behavior has been described in the

Table 4. Grid independence for parabolic shapes, $\mathrm{Ra} = 10^5$, $\epsilon = 0$

Grid	$\overline{\mathrm{Nu}_c}$(C2)	$\overline{\mathrm{Nu}_c}$ (C4)
21×41	4.070	3.231
31×61	4.253	3.198
41×81	4.282	3.185
51×101	4.308	3.187

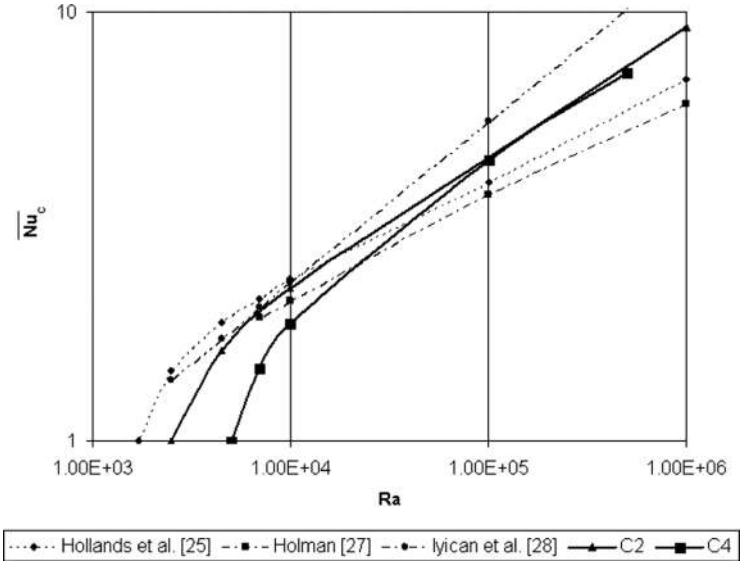

Figure 4. Pure convection Nusselt number comparison. Correlations by Hollands et al. [25], Holman [27], and Iyican et al. [28] compared to parabolic cavities with concentration levels C2 and C4.

past by a number of authors analyzing enclosures with regular geometries [6–8]. The average radiative Nusselt number for this cavity is shown in Figure 5*b*. The sum of $\overline{Nu_c}$ and $\overline{Nu_r}$ for $\epsilon = 1$ is larger than the value of $\overline{Nu_c}$ for $\epsilon = 0$. A similar behavior is obtained for a cavity with a level of concentration C4 as shown in Figures 5*c* and 5*d*. The difference between the convective Nusselt numbers for $\epsilon = 0$ and $\epsilon = 1$ is larger for this level of concentration, however the overall Nusselt number is larger for the case of combined natural convection and radiation than for natural convection only. It is observed that no steady state solution was obtained for a level of concentration C4 at $\mathrm{Ra} = 1.0 \times 10^6$.

4.2.2. Effect of emissivity on temperature distribution and stream function. The effect of emissivity on natural convection inside the parabolic cavity was also studied. For the sake of brevity the simulations were performed only for a level of concentration C4. In Figure 6 the dimensions of the cavity have been normalized with respect to the distance between the hot and the cold walls. The effect of emissivity on the isotherms is shown for a Rayleigh number $\mathrm{Ra} = 1.0 \times 10^5$, reference temperature $T_0 = 293.5\,\mathrm{K}$, and a temperature ratio $\theta_0 = 2.935$. The emissivity values in the figure correspond to (*a*) $\epsilon = 0$, (*b*) $\epsilon = 0.1$, (*c*) $\epsilon = 0.5$, and (*d*) $\epsilon = 1.0$, respectively. Surface radiation significantly modifies the temperature distribution inside the cavity. The change of the temperature distribution is significant between pure convection and convection with radiation. As we increase the value of the emissivity, the change in the temperature distribution is less evident. As the emissivity is increased, at this Rayleigh number, the temperature distribution at the bottom of the cavity becomes more uniform and the isotherms become more parallel to

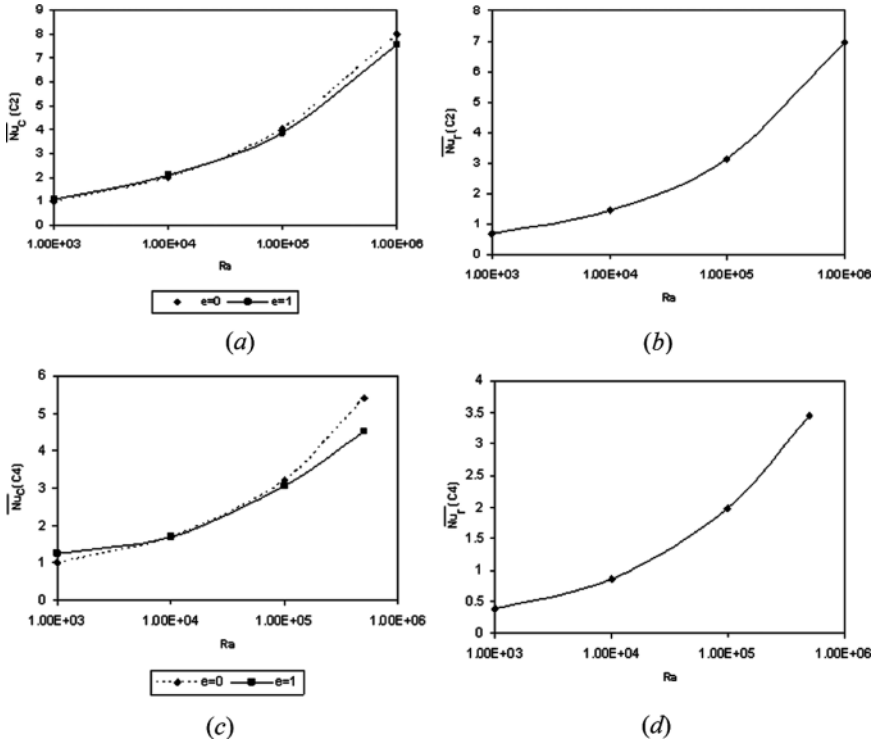

Figure 5. Effect of radiation on convective and radiative Nusselt number ($T_0 = 293.5$ K, $\theta_0 = 2.935$, $\epsilon = 1$).

the hot wall increasing the temperature gradient at the wall. This improves the amount of heat transfer by conduction from the hot wall and the convective Nusselt number increases by 4.9%. As the values of emissivity approach unity, the temperature gradient at the hot wall is reduced and natural convection is also weakened. This behavior is quantified in Figure 7 that shows the average convective and radiative Nusselt numbers calculated at the hot wall. The radiative Nusselt number increases strongly with emissivity. It increases much more than the reduction of the convective Nusselt number so the overall Nusselt number at the bottom of the cavity is larger than for pure natural convection.

The effect of surface radiation on the stream function is shown in Figure 8. There are no major qualitative changes in the streamlines as we increase the emissivity but the intensity of the flow is varied. The maximum value of $|\psi|$ decreases with the emissivity.

4.2.3. Effect of emissivity on Nu_{cH} and Nu_{cC}. The local values of the convective Nusselt number calculated along the hot wall are plotted in Figure 9. It is evident that the value of the emissivity has a strong effect on the local values of Nu_{cH}. The maximum value of the Nusselt number for convection with no radiation is 4.73 and is located at $x/S = 0.63$. On the other hand, the maximum value

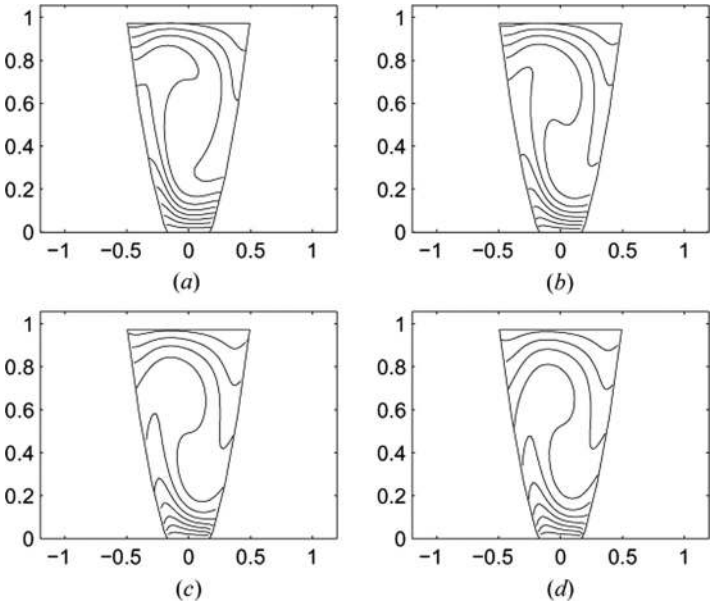

Figure 6. Effect of emissivity on temperature. (*a*) $\epsilon = 0$, (*b*) $\epsilon = 0.1$, (*c*) $\epsilon = 0.5$, and (*d*) $\epsilon = 1.0$ ($\mathrm{Ra} = 10^5$, $T_0 = 293.5$ K, $\theta_0 = 2.935$).

of Nu_{cH} is 5.78 for $\epsilon = 0.1$, and 6.56 for $\epsilon = 1$ and they are both located at $x/S = 1$. It is also seen that for most of the length of the absorber the local values of Nu_{cH} for $\epsilon = 0.1$ are larger than the values for $\epsilon = 0$ and $\epsilon = 1$. Therefore, the average value of the convective Nusselt number at the hot wall is larger for $\epsilon = 0.1$ than for the other two cases.

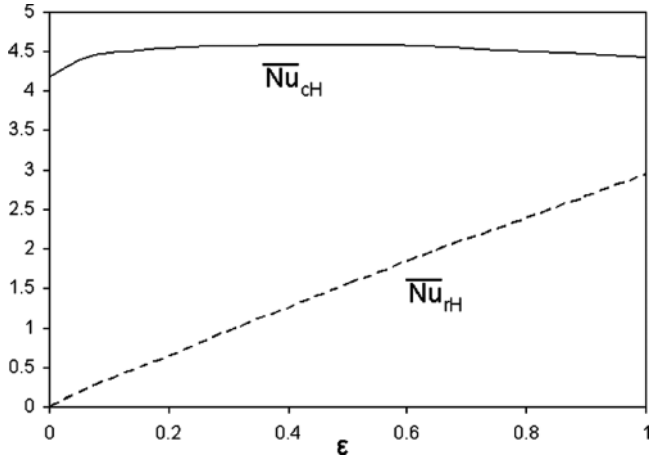

Figure 7. Effect of emissivity on average convective and radiative Nusselt numbers at the bottom of the cavity. Solid line is $\overline{\mathrm{Nu}_{cH}}$ and dashed line is $\overline{\mathrm{Nu}_{rH}}$ ($\mathrm{Ra} = 10^5$, $T_0 = 293.5$ K, $\theta_0 = 2.935$).

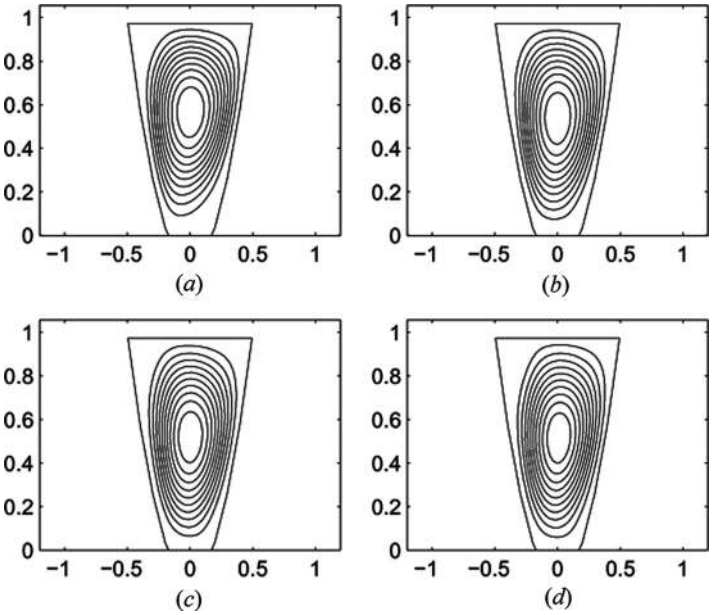

Figure 8. Effect of emissivity on streamlines. (*a*) $\epsilon = 0$, (*b*) $\epsilon = 0.1$, (*c*) $\epsilon = 0.5$, and (*d*) $\epsilon = 1.0$ ($Ra = 10^5$, $T_0 = 293.5$ K, $\theta_0 = 2.935$).

The local values of the convective Nusselt number along the cold wall are plotted in Figure 10. It is seen that the values do not differ significantly between the cases of pure natural convection and $\epsilon = 0.1$. However, the local values of Nu_{cC} for $\epsilon = 1$ are, in general, much lower than for the other two cases. The maximum

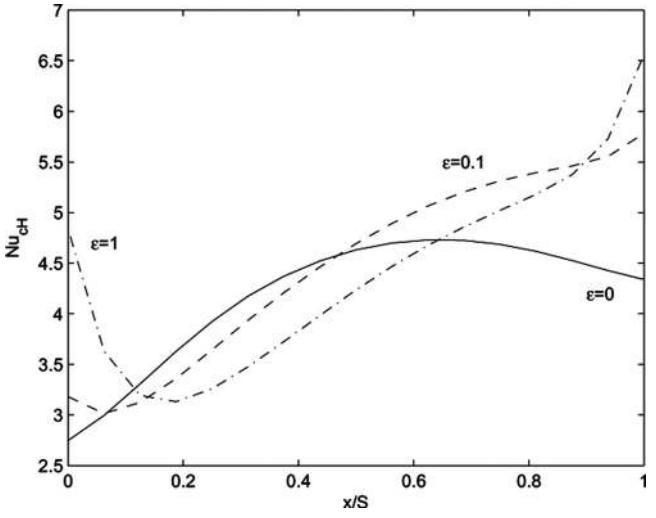

Figure 9. Effect of emissivity on Nu_{cH}. $\epsilon = 0$: —, $\epsilon = 0.1$: - -, and $\epsilon = 1$: -.- ($Ra = 10^5$, $T_0 = 293.5$ K, $\theta_0 = 2.935$).

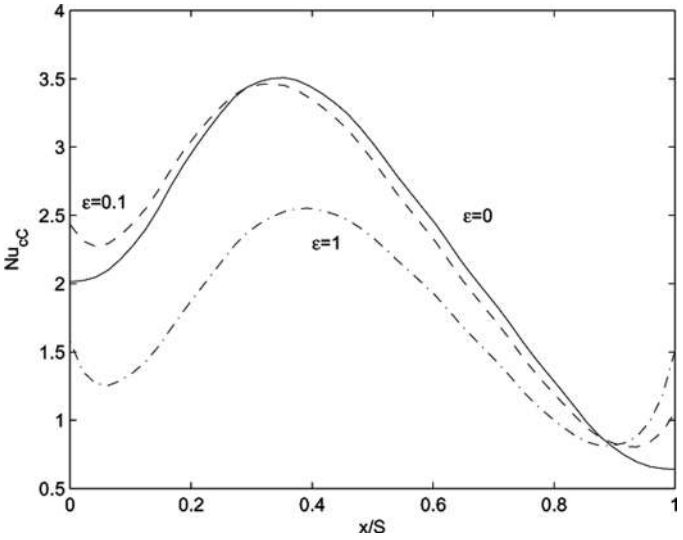

Figure 10. Effect of emissivity on Nu_{cC}. $\epsilon = 0$: —, $\epsilon = 0.1$: --, and $\epsilon = 1$: -.- ($Ra = 10^5$, $T_0 = 293.5$ K, $\theta_0 = 2.935$).

value of Nu_{cC} for pure convection is 3.51 compared to 2.55 for $\epsilon = 1$. The average value of Nu_{cC} for the $\epsilon = 1$ case is 25.2% lower than for pure convection. This offsets the 6.1% increase of Nu_{cH} for $\epsilon = 1$ with respect to natural convection only. Thus, the overall average of Nu_c for the hot and cold walls is larger for pure convection than for convection with radiation at $\epsilon = 1$. This is in agreement with the plots shown in Figure 5.

5. CONCLUSIONS

The effect of surface radiation on natural convection inside parabolic cavities heated from below has been studied numerically. These cavities arise in the design of non-imaging optics-based concentrators. To the best of our knowledge, no other study has addressed the combined effects of natural convection and radiation in this geometry. A coordinate transformation that converts the physical domain into a computational domain is used to solve the governing equations. Two different levels of concentration are analyzed. The results show that when radiation is neglected the onset of fluid motion is delayed by the level of concentration of the cavity. When radiation is considered, it has an important effect on the temperature distribution inside the parabolic cavities, as well as the local and average values of the convective and radiative Nusselt numbers. The emissivity has a strong effect on the average radiative Nusselt number especially at high Rayleigh numbers. On the other hand, it has a weak effect on the average convective Nusselt number calculated at both, the hot and cold walls. The value of $\overline{Nu_c}$ is slightly higher for pure convection than for convection with radiation at $\epsilon = 1$, but the sum of the average convective and radiative Nusselt numbers is larger than the value of $\overline{Nu_c}$ for pure convection.

REFERENCES

1. G. De Vahl Davis, Natural Convection of Air in a Square Cavity: A Bench Mark Numerical Solution, *Int. J. Num. Meth. Fluids*, vol. 3, pp. 249–264, 1983.
2. G. De Vahl Davis and I. P. Jones, Natural Convection in a Square Cavity: A Comparison Exercise, *Int. J. Num. Meth. Fluids*, vol. 3, pp. 227–248, 1983.
3. D. C. Wan, B. S. B. Patnaik, and G. W. Wei, A New Benchmark Quality Solution for the Buoyancy-Driven Cavity by Discrete Singular Convolution, *Numer. Heat Transfer B*, vol. 40, pp. 199–228, 2001.
4. V. Bubnovich, C. Rosas, R. Santander, and G. Caceres, Computation of Transient Natural Convection in a Square Cavity by an Implicit Finite-Difference Scheme in Terms of the Stream Function and Temperature, *Numer. Heat Transfer A*, vol. 42, pp. 401–425, 2002.
5. M. Rahman and M. A. R. Sharif, Numerical Study of Laminar Natural Convection in Inclined Rectangular Enclosures of Various Aspect Ratios, *Numer. Heat Transfer A*, vol. 44, pp. 355–373, 2003.
6. C. Balaji and S. P. Venkateshan, Interaction of Surface Radiation with Free Convection in a Square Cavity, *Int. J. Heat Fluid Flow*, vol. 14, no. 3, pp. 260–267, 1993.
7. M. Akiyama and Q. P. Chong, Numerical Analysis of Natural Convection with Surface Radiation in a Square Enclosure, *Numer. Heat Transfer A*, vol. 31, pp. 419–433, 1997.
8. E. H. Ridouane, M. Hasnaoui, A. Amahmid, and A. Raji, Interaction between Natural Convection and Radiation in a Square Cavity Heated from Below, *Numer. Heat Transfer A*, vol. 45, pp. 289–311, 2004.
9. E. H. Ridouane, M. Hasnaoui, and A. Campo, Effects of Surface Radiation on Natural Convection in a Rayleigh-Benard Square Enclosure: Steady and Unsteady Conditions, *Heat Mass Transfer*, vol. 42, pp. 214–225, 2006.
10. S. Jaballah, H. Sammouda, and A. Belghith, Effect of Surface Radiation on the Natural-Convection Stability in a Two-Dimensional Enclosure with Diffusely Emitting Boundary Walls, *Numer. Heat Transfer A*, vol. 51, pp. 495–516, 2007.
11. K. Slimi, A. Mhimid, M. Ben Salah, S. Ben Nasrallah, A. A. Mohamad, and L. Storesletten, Anisotropy Effects on Heat and Fluid Flow by Unsteady Natural Convection and Radiation in Saturated Porous Media, *Numer. Heat Transfer A*, vol. 48, pp. 763–790, 2005.
12. A. W. Date, Numerical Prediction of Natural Convection Heat Transfer in Horizontal Annulus, *Int. J. Heat Mass Transfer*, vol. 29, no. 10, pp. 1457–1464, 1986.
13. N. Wansophark, A. Malatip, and P. Dechaumphai, Streamline Upwind Finite Element Method for Conjugate Heat Transfer Problems, *Acta Mech. Sinica*, vol. 21, pp. 436–443, 2005.
14. H. M. Badr and K. Shamsher, Free Convection from an Elliptic Cylinder with Major Axis Vertical, *Int. J. Heat Mass Transfer*, vol. 36, no. 14, pp. 3593–3602, 1993.
15. Y. E. Karyakin, Transient Natural Convection in Prismatic Enclosures of Arbitrary Cross-Section, *Int. J. Heat Mass Transfer*, vol. 32, no. 6, pp. 1095–1103, 1989.
16. T. S. Lee, Computational and Experimental Studies of Convective Fluid Motion and Heat Transfer in Inclined Non-Rectangular Enclosures, *Int. J. Heat Fluid Flow*, vol. 5, no. 1, pp. 29–36, 1984.
17. N. U. Aydemir, A. C. M. Sousa, and J. E. S. Venart, Transient Laminar Free Convection in Horizontal Cylinders, *Warme-und Stoffubertagung*, vol. 20, pp. 59–67, 1986.
18. S. I. Abdel-Khalik, H. Li, and K. R. Randall, Natural Convection in Compound Parabolic Concentrators - A Finite-Element Solution, *J. Heat Transfer*, vol. 100, pp. 199–204, 1978.
19. R. A. Tatara and T. Thodos, Experimental Natural Convective Studies within a Compound Parabolic Concentrator Enclosure, *ASME HTD*, vol. 39, pp. 199–204, 1984.

20. T. C. Chew, N. E. Wijeysundera, and A. O. Tay, Experimental Study of Free Convection in Compound Parabolic Concentrator (CPC) Cavities, *ASME J. Solar Energy Eng.*, vol. 110, pp. 293–298, 1988.
21. X. Cui and B. Q. Li, A Discontinuous Finite-Element Formulation for Radiative Transfer in Axisymmetric Finite Cylindrical Enclosures and Coupling with Other Mode Heat Transfer, *Numer. Heat Transfer B*, vol. 48, pp. 317–344, 2005.
22. N. Bianco, L. Langellotto, O. Manca, and V. Naso, Numerical Analysis af Radiative Effects on Natural Convection in Vertical Convergent and Symmetrically Heated Channels, *Numer. Heat Transfer A*, vol. 49, pp. 369–391, 2006.
23. R. Winston, Principles of Solar Concentrators of a Novel Design, *Solar Energy*, vol. 20, pp. 59–67, 1974.
24. H. C. Hottel and A. F. Sarofim, *Radiative Heat Transfer*, McGraw-Hill, New York, 1967.
25. K. G. T. Hollands, G. D. Raithby, and L. Konicek, Correlation Equations for Free Convection Heat Transfer in Horizontal Layers of Air and Water, *Int. J. Heat Mass Transfer*, vol. 18, pp. 879–884, 1975.
26. O. G. Martynenko and P. P. Khramtsov, *Free-Convective Heat Transfer*, Springer, New York, 2005.
27. J. P. Holman, *Heat Transfer*, 8th ed., McGraw-Hill, New York, 1997.
28. L. Iyican, L. C. Witte, and Y. Bayazitoglu, An Experimental Study of Natural Convection in Trapezoidal Enclosures, *J. Heat Transfer*, vol. 102, pp. 648–653, 1980.
29. I. Catton, The Effect of Insulating Vertical Walls on the Onset of Motion in a Fluid Heated from Below, *Int. J. Heat Mass Transfer*, vol. 15, pp. 665 –672, 1972.